PALEOCEANOGRAPHY, VOL. 21, PA2021, doi:10.1029/2005PA001247, 2006

Ice sheet action versus reaction: Distinguishing between Heinrich events and Dansgaard-Oeschger cycles in the North Atlantic

Shawn J. Marshall[1] and Michelle R. Koutnik[2]

Received 17 November 2005; revised 28 February 2006; accepted 14 March 2006; published 29 June 2006.

[1] Glaciers and ice sheets play an active role in the climate system and the global hydrological cycle. The stability of continental ice sheets must be better understood for assessments of future sea level rise and to uncover the causes of millennial-scale climate variability that characterized the last glacial period. Ice-rafted debris (IRD) in the midlatitude oceans and subpolar seas tells of widespread calving of icebergs from the Northern Hemisphere ice sheets during the last glacial period, but the climatic implications of this IRD are unclear. Does the sediment record indicate repeated dynamical collapse of the ice sheets, with ice sheets actively forcing the climate system? Alternatively, were ice sheet margins simply advancing and retreating in response to climate vacillations? On the basis of simulations of iceberg delivery to the ocean during the last glacial cycle we argue that the marine record exemplifies both of these phenomena. Heinrich events were clearly episodes of internal dynamical instability of the Laurentide Ice Sheet, while millennial-scale IRD is more simply interpreted as a response of the circum-Atlantic ice sheets to Dansgaard-Oeschger climate cycles. Ice sheets in different coastal regions respond differently to climate fluctuations, but overall iceberg fluxes increase in cold periods, peaking within a few centuries of climatic cooling. Regions with relatively warm, wet climates (Scandinavia, western North America, and Svalbard) are the most sensitive to millennial climate variability, with rapid response times and large millennial variability in iceberg fluxes.

Citation: Marshall, S. J., and M. R. Koutnik (2006), Ice sheet action versus reaction: Distinguishing between Heinrich events and Dansgaard-Oeschger cycles in the North Atlantic, *Paleoceanography*, *21*, PA2021, doi:10.1029/2005PA001247.

1. Introduction

[2] The question of whether continental ice sheets are intrinsically unstable, prone to dynamical collapse, is critical to predictions of global sea level rise in the decades and centuries ahead, as the Greenland and Antarctic Ice Sheets adapt to ongoing climate change [e.g., *Church and Gregory*, 2001]. Ice sheets respond to atmospheric and oceanic conditions through accumulation and ablation of snow and ice, calving of ice at marine-based margins, and basal melting beneath floating ice shelves. These mechanisms can be classified as mass balance controls on ice sheet advance and retreat. Glacier-climate models are generally able to capture the mass balance response of ice sheets to changing temperature and precipitation regimes [e.g., *Ohmura et al.*, 1996; *Gregory and Oerlemans*, 1997; *Huybrechts and de Wolde*, 1999], although uncertainties arise because of the emerging understanding that glaciological responses to climate change will not be linear. For example, ice shelf breakup [*Vaughan and Doake*, 1996; *Scambos et al.*, 2000] and meltwater-lubricated basal flow are threshold processes that lead to accelerated ice sheet flow and increased ice sheet sensitivity to climate warming [*Zwally et al.*, 2004; *Rignot et al.*, 2004; *Parizek and Alley*, 2004].

[3] While parameterizations of these mass balance processes need to be refined in ice sheet models, their potential impact on sea level rise can be estimated [*Church and Gregory*, 2001; *Gregory and Oerlemans*, 1997; *Huybrechts and de Wolde*, 1999]. Internal dynamical instabilities in glaciers and ice sheets are another matter. Surges of valley glaciers and ice cap outlets are commonplace and are well documented [*Clarke*, 1987; *Björnsson et al.*, 2003], but the subglacial controls of surge instabilities are not fully understood. For this reason, parameterizations of surge dynamics as well as fast flowing ice streams are absent or unreliable in current ice sheet models [*Marshall et al.*, 2000]. Although such instabilities are theoretically predicted in continental ice sheets, it is unknown whether the Greenland and Antarctic Ice Sheets are vulnerable to dynamical instabilities analogous to those observed in glaciers and ice caps [*MacAyeal*, 1993; *Marshall and Clarke*, 1997]. If a surge event destabilizes a large area of an ice sheet, it is capable of tapping into a vast reservoir of inland ice and generating significant sea level impacts on decadal and centennial timescales. Heinrich events testify to precisely this type of dynamical instability in the Laurentide Ice Sheet (LIS) during the last glaciation.

[1]Department of Geography, University of Calgary, Calgary, Alberta, Canada.
[2]Department of Earth and Space Sciences, University of Washington, Seattle, Washington, USA.

0883-8305/06/2005PA001247$12.00

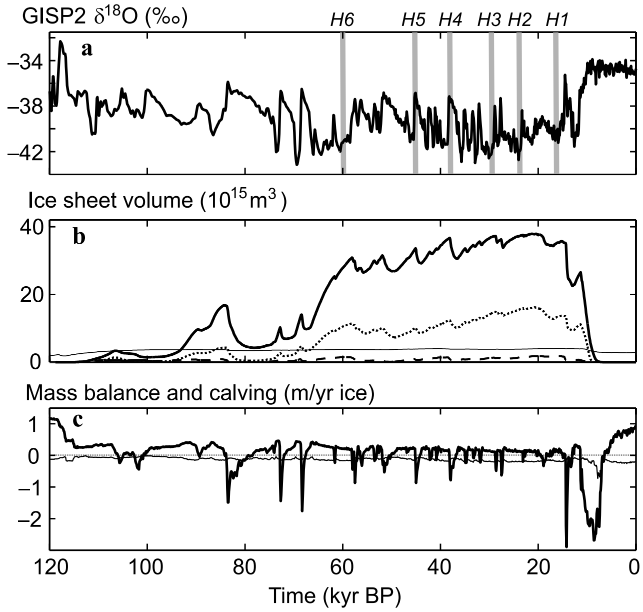

Figure 1. (a) The $\delta^{18}O$ forcing for the last glacial cycle from the Greenland Ice Sheet Project 2 (GISP2) ice core (‰) [*Grootes et al.*, 1993]. Heinrich events are indicated at 60, 45, 36, 28, 23 and 16 kyr B.P., with dates taken from *Hemming* [2004]. (b) Modeled ice sheet volume (10^{15} m^3) in North America (bold solid line), Eurasia (dotted line), Greenland (thin solid line), and Iceland (dashed line). (c) Areally averaged mass balance (thick solid line) and calving rates (thin solid line) for the North American ice sheets (m/yr ice equivalent). Mass balance, b, is net accumulation minus losses due to melting and calving. The dotted line indicates $b = 0$, the condition for a steady state ice sheet.

1.1. Heinrich Events

[4] *Heinrich* [1988] identified layers with high percentages of coarse lithic grains in oceanic sediment cores from the North Atlantic. These large, unweathered lithic clasts must have been delivered to the open ocean by iceberg release or sea ice drift, and are hence termed ice-rafted detritus (IRD). The six dominant IRD layers in the North Atlantic were subsequently dated between 60–16 kyr B.P. [*Bond et al.*, 1992, 1993] and are referred to as Heinrich events H6 to H1 (Figure 1a). *Hemming* [2004] provides a detailed review of the paleoceanographic record of Heinrich events; we provide a brief summary here, with an emphasis on their implications for ice sheet behavior.

[5] As discussed by *Hemming* [2004], a high percentage of IRD during these events could be due to a high flux of IRD or a low flux of foraminifera. Events H1, H2, H4, and H5 show a high flux of IRD, whereas H3 and H6 appear to be periods of low foraminiferal flux [*Gwiazda et al.*, 1996a; 1996b]. Geochemical analysis of Heinrich layers has determined a Hudson Strait source for grains in H1, H2, H4, and H5 [*Andrews and Tedesco*, 1992; *Grousset et al.*, 1993; *Hemming et al.*, 1998, 2002; *Farmer et al.*, 2003]. However, H3 and H6 could be different [*Gwiazda et al.*, 1996b]. While H3 resembles the other Heinrich events in the Labrador Sea [*Hillaire-Marcel et al.*, 1994; *Stoner et al.*, 1998], its chemical composition in the North Atlantic is enigmatic, suggesting more circum-Atlantic sources [*Gwiazda et al.*, 1996b; *Grousset et al.*, 1993, 2001; *Snoeckx et al.*, 1999]. If H3 corresponds with an ice dynamical instability in Hudson Strait, it may have been muted relative to events H1, H2, H4 and H5. H6 has been less studied [*Hemming*, 2004] and is difficult to compare with the later events. This picture will continue to clarify, but for purposes here the essential message from the North Atlantic is that the last glaciation was characterized by intermittent, episodic fluxes of IRD from the Hudson Strait region, with 4 to 6 of these events over the last 60 kyr.

[6] The age and duration of Heinrich events is difficult to constrain. Estimates range from a few hundred to a few thousand years [*Bond et al.*, 1992, 1993; *Andrews et al.*, 1994; *Francois and Bacon*, 1994; *Thompson et al.*, 1995; *Vidal et al.*, 1997; *Cortijo et al.*, 1997; *McManus et al.*, 1998; *Veiga-Pires and Hillaire-Marcel*, 1999; *Grousset et al.*, 2001]. *Hemming* [2004] provides a thorough review of the timing of Heinrich events and concludes that their average duration can be estimated at 495 ± 255 years. Heinrich events were associated with freshwater dilution, cold surface waters, and disruptions in North Atlantic deepwater formation [e.g., *Broecker*, 1994; *Vidal et al.*, 1997; *Zahn et al.*, 1997; *Elliot et al.*, 2002; *McManus et al.*, 2004]. These events have been noted as being coincident with Northern Hemisphere climate changes seen in the Greenland ice cores [*Bond et al.*, 1993; *Broecker*, 1994] and also appear to have had far-reaching climatic impacts [e.g., *Lowell et al.*, 1995; *Porter and An*, 1995; *Broecker and Hemming*, 2001; *Voelker*, 2002].

[7] Estimates of the total freshwater input to the North Atlantic range from 1–2 m [e.g., *Roche et al.*, 2004] to more than 15 m of global sea level rise over a few hundred years [*Chappell*, 2002; *Siddall et al.*, 2003; *Rohling et al.*, 2004]. *Dowdeswell et al.* [1995] used estimates of total IRD mass in Heinrich layer debris, combined with consideration of typical sediment concentrations in icebergs, to suggest a sea level rise of 0.39 to 3.9 m in Heinrich events, although *Hemming* [2004] notes that their estimate of total IRD mass may be high by a factor of ~2. This would argue for a 0.2–2 m contribution to global sea level, consistent with *Roche et al.* [2004]. The glaciological modeling of *Alley and MacAyeal* [1994] suggests the potential for 0.01 m/yr of sea level rise associated with a 200–300 year period of ice stream activity in Hudson Strait, or a total sea level contribution of 2–3 m. *Hemming* [2004] estimates a sea level rise of 10–20 m for a 500-year event, based on the $\delta^{18}O$ record of freshwater dilution in the North Atlantic, a 50- to 100-m mixed layer, and estimates of the advective input of Gulf Stream water to the North Atlantic current.

[8] There are myriad other ice-rafted deposits in the North Atlantic from the last glacial period [e.g., *Bond and Lotti*, 1995]. However, Heinrich events are clearly distinctive layers that are superimposed on this background IRD flux. Heinrich events most likely represent intermittent ice sheet instabilities in Hudson Strait, as proposed by *MacAyeal* [1993] and supported by glaciological modeling [*Marshall*

and Clarke, 1997; *Calov et al.*, 2002]. In this paper we consider the possibility that millennial-scale variations in ambient IRD are a simple response to mass balance driven, hemisphere-scale ice sheet response to millennial-scale climate variability. This interpretation has also been suggested by *Alley et al.* [1999], *Elliot et al.* [2001] and *Hemming* [2004]; here we test the idea with an ice sheet model.

1.2. Dansgaard-Oeschger Cycles

[9] The last glacial period was characterized by 1- to 3-kyr oscillations between warm interstadials and cold stadials (Figure 1a), known as Dansgaard-Oeschger (D-O) cycles. As documented by the ice core record of central Greenland, D-O cycles featured rapid (decade scale) warming events of 10−15°C followed by a gradual return to deep glacial temperatures [*Johnsen et al.*, 1992; *Dansgaard et al.*, 1993; *Grootes et al.*, 1993]. D-O cycles have a widespread IRD signature and paleoceanographic imprint in the North Atlantic region [*Bond et al.*, 1993; *Bond and Lotti*, 1995; *Dokken and Jansen*, 1999; *Elliot et al.*, 1998, 2001, 2002; *van Kreveld et al.*, 2000]. The timescale of D-O cycles suggests that variations in deepwater circulation play a central role [*Broecker*, 1994], but the oscillations could be internal [e.g., *Rahmstorf*, 2002] or they could be a resonation in response to stochastic [*Alley et al.*, 2001] or freshwater forcing [e.g., *Keigwin et al.*, 1991; *Clark et al.*, 2002].

[10] The degree to which Greenland δ^{18}O records represent temperature variability needs to be better understood. *Denton et al.* [2005] present evidence for large changes in seasonality during the glacial period, with severe cold accentuated in wintertime. This has important implications for our simulations, because glacier mass balance is most sensitive to summer temperatures. Another recent study by *Li et al.* [2005] shows that the isotopic oscillations in Greenland ice cores may be influenced by millennial-scale variability of the extent of the winter sea ice edge, with concomitant impacts on the seasonality of precipitation (hence isotopic signatures) in central Greenland. Hence the true magnitude of temperature changes associated with the D-O cycles may be damped compared to the current interpretation of isotopic variations in Greenland ice cores. However, gas-phase isotope fractionation data from Greenland provides independent evidence that there were large local temperature shifts associated with the δ^{18}O oscillations, at least during the Bølling transition [*Severinghaus and Brook*, 1999]. The Bølling was a major millennial-scale warming event that punctuated the last deglaciation (14.7 kyr B.P.), and it closely resembles the glacial age interstadial warmings in the Summit, Greenland ice cores. We therefore adopt the ice core δ^{18}O record as a proxy for mean annual temperature variations in our simulations, but recognize that summer temperature changes may be overestimated by this assumption [*Denton et al.*, 2005]. Sensitivity tests explore the impact of this assumption on our results.

[11] We do not address the origin of D-O cycles in the simulations presented here. Rather, we ask the simpler question: how did the Northern Hemisphere ice sheets respond to the millennial-scale climate variability that they were subject to? The fundamental nature of mass balance driven ice sheet response to climate change has yet to be resolved. For instance, it is not even clear whether increased iceberg fluxes are expected during periods of ice sheet advance (stadials) or ice sheet decay (interstadials) [*McCabe and Clark*, 1998; *Clarke et al.*, 1999]. To explore this question we run simulations of iceberg delivery to the ocean from the circum-Atlantic ice sheets over the past 120 kyr. Our analysis focuses on the timing and extent of modeled iceberg discharge from different coastal zones.

2. Simulations of the Last Glacial Cycle: Model Design

[12] The last glacial cycle in the Northern Hemisphere is simulated using a model of ice sheet dynamics and thermodynamics that is driven by general circulation model (GCM)- and ice-core-derived climatology for the last 120 kyr [*Marshall et al.*, 2000, 2002]. The model includes simple treatments of floating ice and iceberg calving dynamics, which allow ice to advance onto the continental slope. The model domain is 27°−85°N and 360° in longitude, with a resolution of 0.5° in latitude and 1° in longitude over the whole domain and nested higher-resolution grids for Greenland (1/6° by 1/3°) and Iceland (1/10° by 1/6°).

[13] The ice sheet model solves the 3-D conservation equations for mass, momentum, and energy to predict ice thickness, velocity, and temperature. Temperature influences ice dynamics through the effective viscosity of the ice and the evolution of the basal thermal regime; regions of the ice sheet that are at the melting point at the base are able to undergo basal flow via sliding and sediment deformation. The ice dynamics model is coupled to a viscoelastic Earth model to simulate isostatic adjustments through the glacial cycle [*Marshall et al.*, 2002]. An ice sheet is present in Greenland at the beginning of the simulation (120 kyr B.P.), based on a spin-up simulation of Greenland Ice Sheet evolution from 160 to 120 kyr B.P. [*Marshall and Cuffey*, 2000]. All other regions are prescribed to be ice-free at the beginning of the simulation.

[14] Ice shelf dynamics are simplified in our model. Ice margins that advance onto open water (the continental shelf or an interior water body such as Hudson Bay) will initially float and will be subject to creep thinning and calving at the marine interface. We prescribe calving as a function of ice thickness H and water depth H_w,

$$Q_c = k(T) H H_w, \tag{1}$$

where $k(T)$ is a parameter that decreases with ice temperature T [*Marshall et al.*, 2000]. This approximates the effects of temperature on tensile strength of the floating ice tongue, to empirically capture the higher rates of calving that are known to occur in temperate ice (e.g., tidewater glaciers in Alaska versus Antarctic ice shelves). If floating ice thickens it can ground, promoting further ice advance onto the continental shelf. There is no bathymetric limit on the advance of floating (ice shelf) or grounded ice. Further details regarding model treatment of calving dynamics and grounding-line migration are discussed by *Marshall et al.* [2000].

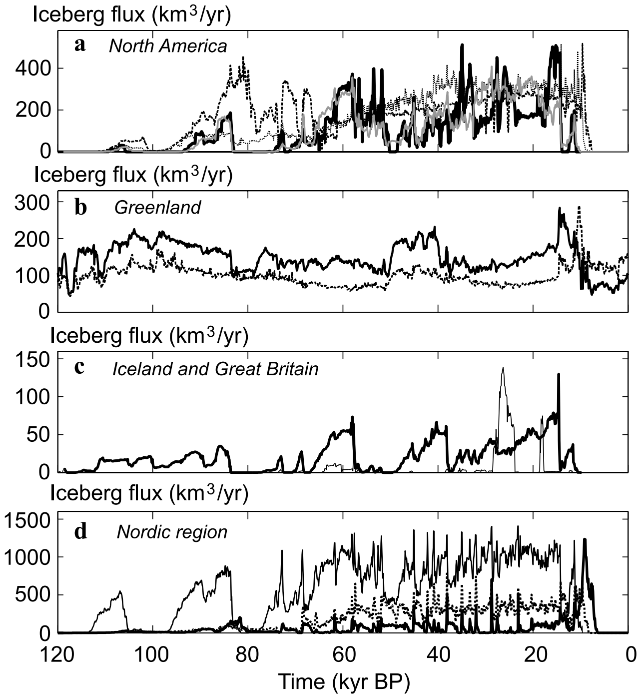

Figure 2. Modeled iceberg flux to the North Atlantic Ocean and subpolar seas from different coastal zones through the last glacial cycle (km^3/yr): (a) Hudson Strait (dashed line), Cabot Strait (thick solid line), Labrador (grey line), and Baffin Bay (dotted line); (b) north Greenland (dashed line) and south Greenland (solid line); (c) Iceland (thick line) and western Europe (thin line); and (d) Scandinavia (thin solid line), Svalbard (dashed line), and the Barents Sea (thick solid line).

[15] Climate forcing for the simulations is based on precipitation and temperature fields from GCM snapshots of present-day and last glacial maximum (LGM) climate [*Vettoretti et al.*, 2000], interpolated onto the model grid. Temporal climate variability is introduced through a "glacial index" derived from the GISP2 ice core δ^{18}O stratigraphy [*Grootes et al.*, 1993]. The δ^{18}O record is resampled to 100-year values and the glacial index time series is translated to a climate forcing through a weighted interpolation of LGM and present-day (interglacial) climate, corrected for changing ice surface elevations during the glacial period. This is a crude climate forcing, but its primary purpose in our numerical experiments is to drive the Northern Hemisphere ice sheets through a glacial-interglacial cycle, including millennial climate variability. The Greenland ice core records are well suited to this end, and uncertainties in the ice core age scales (e.g., discrepancies between GISP2, GRIP, and NGRIP) do not impact the conclusions of our numerical experiments.

[16] More important to our investigation is the concern that isotopic oscillations experienced in Greenland may overestimate temperature variability [e.g., *Li et al.*, 2005; *Denton et al.*, 2005] and will not be representative of hemispheric-scale climate fluctuations. For this reason we do not use the inferred D-O or glacial-interglacial temperature variability from Greenland to drive our climatology; the amplitude of local temperature variability comes from the GCM simulations, which have spatially variable climate perturbations throughout the domain, including (for instance) a muted glacial climate change signal in western North America relative to the North Atlantic region [*Vettoretti et al.*, 2000]. Our greater concern is how much of the D-O isotopic shift in central Greenland represents a temperature signal compared to the effects of varying seasonality of precipitation. Sensitivity tests presented below test the impact of diminishing the amplitude of the millennial climate perturbations during the glacial period.

3. Simulations of the Last Glacial Cycle: Results

[17] Figure 1b plots simulated ice sheet volume over the last 120 kyr from North America, Eurasia, Greenland and Iceland, while Figure 1c shows the average mass balance variability over the North American ice sheets in the simulation. The ice-core-based climate forcing contains large millennial variability, with evident impacts on mass balance. However, the relatively long timescale of continental ice sheet dynamics integrates this high-frequency mass balance variability to give a relatively smooth evolution of total ice sheet volume through the glacial cycle.

[18] Consideration of just the total ice volume obfuscates the systematic, D-O-driven variability at the margins of the ice sheets. Figure 2 plots modeled iceberg flux to the North Atlantic and subpolar seas over the last 120 kyr, based on discrete coastal zones of North America, Greenland, Iceland, and Europe. Our coastal zones are illustrated in Figure 3 and defined in Table 1. They are designed to account for the entire marine margin of the Northern Hemisphere ice sheets, noting that the ice sheet margins migrate with time. Iceberg flux in each coastal zone is the sum of all icebergs that calve to that sector of the ocean, regardless of distance offshore. The millennial variability of iceberg flux to the oceans is evident in Figure 2 and is produced by sequences of ice sheet advance and retreat from the continental shelves/slopes. This reflects the response of the ice sheets to the changing mass balance conditions during D-O cycles; ice margins advance during cold stadials and retreat during warm interstadials. Greenland is the only significant source of Holocene icebergs in the model (Figure 2b), although small fluxes issue from Svalbard and the Canadian Arctic islands (Baffin Bay coastal zone).

[19] Figure 3 plots the integrated iceberg flux from each model grid cell over the entire glacial cycle. Every circum-Atlantic grid cell that experienced calving at some point in the glacial cycle is represented in Figure 3. The width of the calving zones gives an indication of the moving margin of the ice sheet through time, as only ice marginal cells are able to calve. Submarine channels show up clearly in eastern North America and the Norwegian Sea; these are areas where ice flux was concentrated, with thick ice and high velocities combining to produce high rates of calving. Table 2 summarizes this integrated iceberg flux for each of our coastal zones. The "normalized" iceberg flux from each

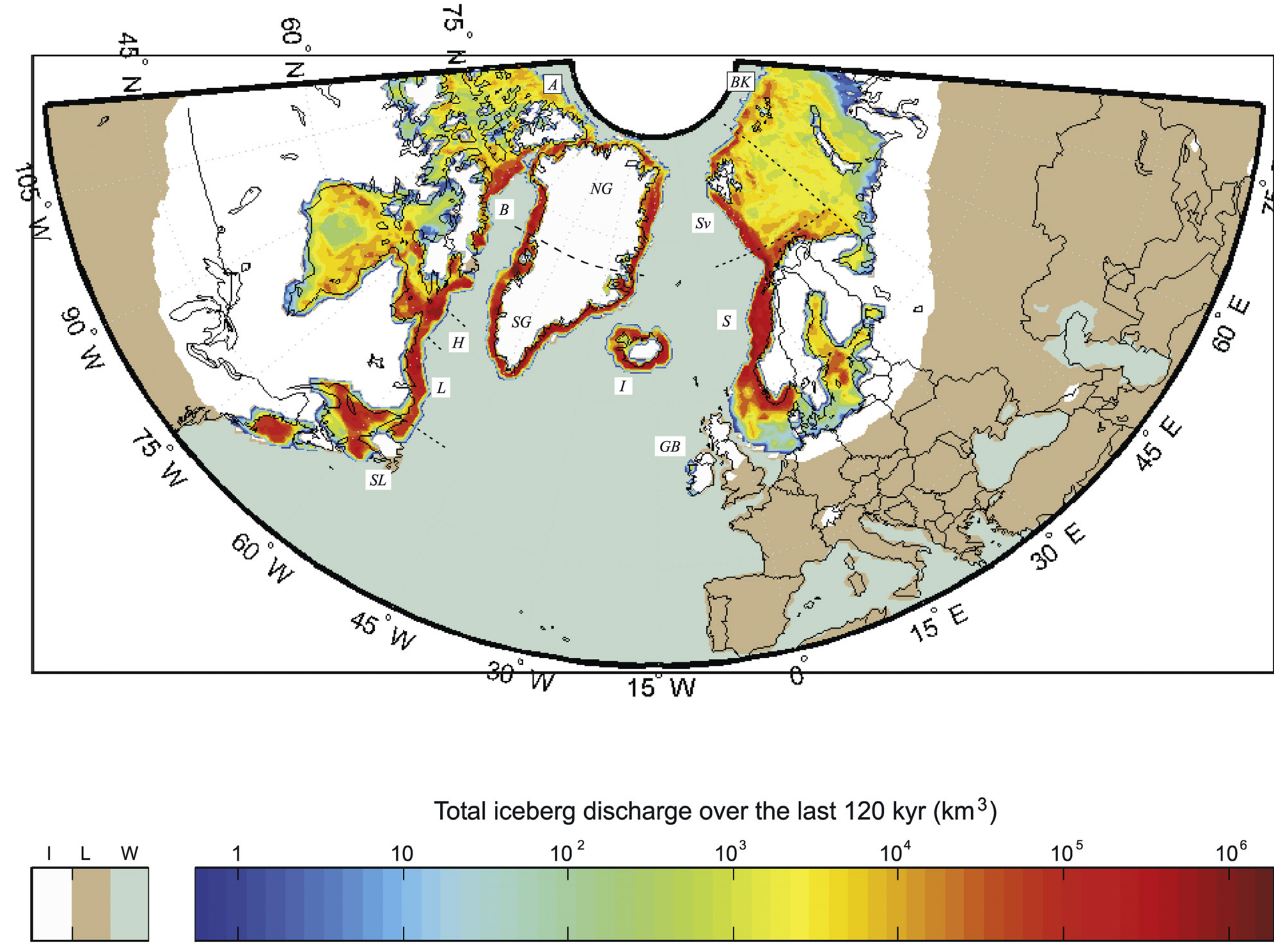

Figure 3. Cumulative iceberg flux from the circum-North Atlantic ice sheets through the last glacial cycle (120 kyr B.P. to present) (km^3). Contours are plotted on a log scale. The plot indicates all areas that experienced iceberg calving in the last 120 kyr. Areas in white indicate the modeled last glacial maximum (21 kyr B.P.) ice sheets in all locations where no icebergs originated.

coastal zone is calculated from the total 120-kyr discharge divided by the approximate length of the coastline for each zone. Note that this is not the true geographical coastline but the breadth of the numerical model grid cells across which iceberg fluxes are delivered to the oceans.

[20] The total modeled iceberg discharge into the North Atlantic and its adjacent subpolar seas was 180.3×10^6 km^3 through the last glacial cycle, with a maximum 100-year discharge of 4375 km^3/yr. This peak discharge is equivalent to 0.12×10^6 m^3/s (Sv) of freshwater forcing. For the period 60–20 kyr B.P., the main phase of the last glaciation, mean iceberg discharge to the entire North Atlantic basin was 2251 km^3/yr (0.06 Sv), which compares with 855 km^3/yr (0.02 Sv) to the North Pacific and 201 km^3/yr (0.005 Sv) to the Arctic basin.

[21] The model predicts intensive iceberg delivery to the oceans from three main sectors of the Northern Hemisphere: the Cordilleran Ice Sheet in western North America, the Scandinavian Ice Sheet, and Hudson Strait. Significant contributions also originate from the southeastern Laurentide Ice Sheet, the Labrador coast, Svalbard, and the marine-based ice sheet in the Barents/Kara Seas. Column 4 of Table 2, $r_{\delta Q}$, indicates the correlation between the GISP2 isotopic (climate) forcing and the iceberg flux Q for the full glacial cycle in each coastal zone. Negative correlations indicate the association of high iceberg fluxes with cold periods. On the 120-kyr (orbital) timescale, this is an unsurprising confirmation that icebergs peak during the glaciation while the interglacial period is relatively iceberg-free. The story becomes more interesting on millennial timescales.

3.1. Ice Margin Response to D-O Cycles

[22] Figure 4 presents a more detailed view of the period 60–20 kyr B.P. for select coastal zones and gives evidence of the rich range of behavior from different sectors of the ice sheets. The GISP2 ice core forcing is shown in Figure 4a [*Grootes et al.*, 1993], while Figure 4b provides an example of the regional temperature variability driven by this forcing, for the southeastern Laurentide Ice Sheet (the ice-covered area in the region 35°N–52°N, 75°W–55°W). In general there are three systematic classes of ice margin

Table 1. Coastal Zones Used to Calculate Regional Iceberg Fluxes

Coastal Zone	Longitude Range	Latitude Range
North Pacific	165°W–120°W	35°N–60°N
Bering Sea	165°W–139°W	60°N–71°N
Canadian Arctic	165°W–139°W	71°N–85°N
	85°W–80°W	70°N–85°N
	72°W–70°W	63°N–70°N
Baffin Bay	80°W–45°W	70°N–85°N
	70°W–45°W	63°N–70°N
Hudson/Foxe Basins[a]	95°W–85°W	51°N–67°N
	85°W–72°W	51°N–70°N
	72°W–65°W	51°N–63°N
	65°W–45°W	60°N–63°N
Labrador	65°W–45°W	52°N–60°N
Southeast Laurentide	75°W–45°W	35°N–52°N
North Greenland	75°W–5°W	71°N–85°N
South Greenland	45°W–5°W	57°N–71°N
Iceland	2°E–30°E	57°N–72°N
Great Britain	10°W–2°E	50°N–61°N
North Sea	2°E–10°E	50°N–57°N
Scandinavia	2°E–30°E	57°N–72°N
Svalbard[b]	10°W–35°E	72°N–85°N
Barents/Kara Seas[b]	35°E–95°E	65°N–85°N
Laptev/Siberian Seas	95°E–180°E	66°N–85°N

[a]The Hudson Strait outlet cells in Table 1 include all icebergs generated in Hudson Bay and the Foxe Basin, so the high normalized flux through Hudson Strait may be exaggerated. Icebergs originating from Hudson Bay and the Foxe Basin are routed to the Labrador Sea via Hudson Strait, so it does act as a throttle; however, some of the icebergs from the interior regions will not have survived to reach the continental slope off of Hudson Strait. Even if these icebergs melted prior to their exodus through the Strait, however, their fresh water will have flooded the Labrador Sea via this coastal zone.

[b]Svalbard and the Barents/Kara Sea regions could be combined, as these ice masses were confluent at the Last Glacial Maximum; we have separated the contributions from these two source regions because there were times when the ice masses were distinct (e.g., the modern state, with active ice masses in Svalbard as well as Novaya Zemlya in the Barents Sea).

response to D-O cycles: (1) regions where iceberg flux increases during the cold phase of the D-O cycles (e.g., Scandinavia, Iceland, southeast Laurentide), (2) regions where iceberg flux peaks during warm episodes (e.g., the marine-based ice caps in Svalbard and the Barents/Kara Seas), and (3) regions that are ambivalent to D-O cycles (e.g., Greenland, the Canadian Arctic).

[23] This generalized behavior reflects ice dynamical timescales and the importance of mean regional climatology in governing ice sheet response to climate perturbations. In the Canadian Arctic, for instance, conditions are almost always too cold for the high-latitude ice sheets to respond to interstadial warmth; there is little or no melt at these latitudes during any stage of the glacial period. D-O cycles therefore have little effect on the margins of the ice sheet in this sector, and therefore little effect on iceberg delivery to the Arctic or to Baffin Bay during the glacial period. Changing precipitation rates create a modest high-latitude response to the millennial climate forcing, but this is minor relative to the temperature sensitivity of most coastal zones.

[24] We argue that behavioral regimes 1 and 2 are actually indicative of the same mode of temperature-driven mass balance response. Ice sheet margins in Scandinavia, the Barents/Kara Seas, and western North America are exceptionally sensitive in our simulations and analysis of these sectors explains this mass balance response. These are regions with relatively mild conditions and high precipitation rates, making the ice sheets very responsive to interstadial warmth. The ice margins withdraw from the coast during warm periods in these regions, producing an initial flush of icebergs when the ice sheets collapse. This is most dramatic from the marine-based ice cap in the Barents/Kara Seas. Retreat from the coastal areas is followed by a period of diminished iceberg flux to the oceans. This is seen in all sub-Arctic coastal zones. During ensuing cold stadials, ice margins readvance onto the continental shelf/slope and calving resumes. Iceberg fluxes then increase throughout the stadial phases, although the timescales of ice sheet advance and retreat differ in each coastal zone.

[25] To focus on the D-O response of the ice sheets during the glacial period, Table 2 presents correlations between iceberg discharge (Q) and GISP2 δ^{18}O for the period 60–

Table 2. Iceberg Statistics Through the Last Glacial Cycle for Northern Hemisphere Coastal Regions[a]

Coastal Zone	Total Iceberg Flux, 10^6 km^3	Normalized Flux, 10^3 km^2	$r_{\delta Q}$, 120 kyr	$r_{\delta Q}$ ($\tau = 0$), 60–20 kyr B.P.	$r_{\delta Q}$ (max), 60–20 kyr B.P.	Lag, year
North Pacific	52.7	19.8	−0.66	−0.52	−0.88	400
Canadian Arctic	13.7	4.2	−0.31	−0.38	−0.50	1000
Baffin Bay	16.8	6.9		−0.51	−0.21	700
Hudson Strait	18.3	54.9	−0.34	−0.23	−0.47	700
Labrador	11.5	12.9	−0.58	−0.38	−0.67	800
Southeast Laurentide	11.0	8.2	−0.48	−0.16	−0.43	600
North Greenland	12.1	4.0	0.42	0.12	0.37	2800
South Greenland	17.8	7.1	−0.32	0.08	0.26	3000
Iceland	2.2	1.6	−0.61	−0.47	−0.59	300
Great Britain	0.5	0.4	−0.22	−0.21	−0.69	400
Scandinavia	62.7	37.7	−0.69	−0.28	−0.80	500
Svalbard	19.8	14.9	−0.34	0.31	0.37	100
Barents/Kara Seas	7.6	3.6	0.28	0.50	0.68	200
Laptev/Siberian Seas	1.6	0.5	−0.11	0.19	0.34	200
Full North Atlantic	180.3	9.3	−0.57	−0.17	−0.68	600

[a]Normalized iceberg flux from each coastal zone (third column) is calculated from the total 120-kyr discharge (km^3 of ice) divided by the length of the coastline for each zone (km). Fourth column indicates the linear correlation between the climate forcing time series (GISP2 δ^{18}O) and iceberg flux (Q) for the full glacial cycle, while fifth and sixth columns indicate this correlation for the time period 60–20 kyr B.P. (with no lag, $\tau = 0$, and for the maximum lagged correlation). The time lag for this maximum correlation is given in last column.

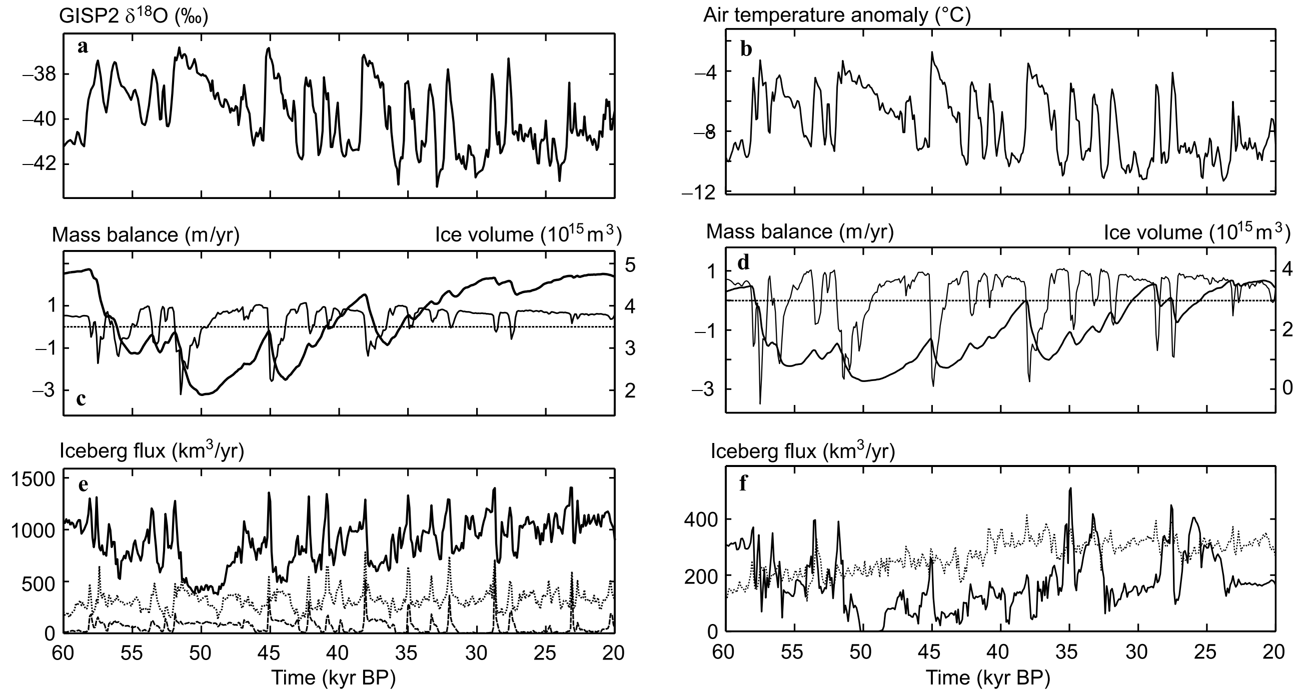

Figure 4. Climatic conditions, ice sheet response, and iceberg flux in northwestern Europe and eastern North America from 60 to 20 kyr B.P. (a) GISP2 $\delta^{18}O$ forcing during this period (‰). (b) Air temperature anomaly (difference from present) in the southeastern sector of the Laurentide Ice Sheet (°C). (c) Mass balance (thin line and left axis, m/yr ice equivalent) and ice sheet volume (thick line and right axis, 10^{15} m^3) in the Scandinavian sector of the Eurasian ice sheet. (d) Mass balance (thin line and left axis, m/yr ice equivalent) and ice sheet volume (thick line and right axis, 10^{15} m^3) in the southeastern (Cabot Strait) sector of the Laurentide Ice Sheet. (e) Iceberg flux from Scandinavia (solid line) and Svalbard (dotted line) and in the Barents/Kara Seas (dashed line) (km^3/yr). (f) Iceberg flux from the southeast Laurentide (solid line) and Baffin Bay (dotted line) (km^3/yr).

20 kyr B.P., including the maximum lagged correlation of iceberg flux and $\delta^{18}O$ in each region. As above, negative numbers indicate peak calving during cold intervals, while positive numbers indicate that warming induces calving. The total circum-Atlantic response is included at the bottom of this table and it indicates that maximum iceberg delivery occurs during the cold phase of the D-O cycles, with a time lag of 600 years from the peak cooling. This reflects the superimposed response of the majority of coastal zones, and the circum-Atlantic signal is particularly dominated by the behavior of the Scandinavian ice sheet in our simulations. Peak iceberg flux lags the cooling because of the delay in ice sheet advance to the coast. Ice margins in Svalbard, the Barents/Kara Seas, and the Siberian shelf exhibit the opposite behavior, as discussed above: a brief and rapid increase in iceberg flux during warm periods. This flushing of icebergs during interstadial retreats in these regions indicates that marine-based ice sheets are more prone to dynamical collapse than their terrestrial brethren (e.g., Scandinavia) and have a longer recovery time for readvance onto the continental shelf.

[26] Figure 5 plots correlations as a function of lag for several regions, illustrating the range of behavior in different climatic and physiographic settings. The brief pulse of icebergs during the onset of the D-O warm phase occurs in most sub-Arctic coastal regions (e.g., Figures 4e and 4f), but only dominates $r_{\delta Q}$ in Svalbard and the Barents/Kara Seas (grey lines in Figure 5). The strongest negative correlations are predicted for western North America and Scandinavia, where steep terrain and high precipitation rates lead to a rapid and spirited ice sheet response to cooling (Figure 4e and dashed lines in Figure 5). Ice margin response in most other sub-Arctic regions is similar to that of Scandinavia, but with less climatic sensitivity and longer response times for the eastern flanks of the Laurentide Ice Sheet.

[27] Greenland is enigmatic in our simulations, showing little overall climate sensitivity. Ice margins in Greenland are advanced to the continental shelf through most of the glaciation, which explains their lack of sensitivity to stadial periods. Greenland's weak sensitivity to interstadial warmth differs from that in the Barents/Kara Sea sector, however; there is no brief flush of icebergs associated with rapid collapse of marine margins. In contrast, warm periods are associated with a weak and long-lived increase in iceberg flux. We interpret this as a response to increases in accumulation that accompany warm periods. There is a relatively long timescale for advection of this mass balance perturbation from the interior of the ice sheet to the ice margins. Overall, however, the signal from Greenland is weak in our simulations, with low variability in iceberg flux from

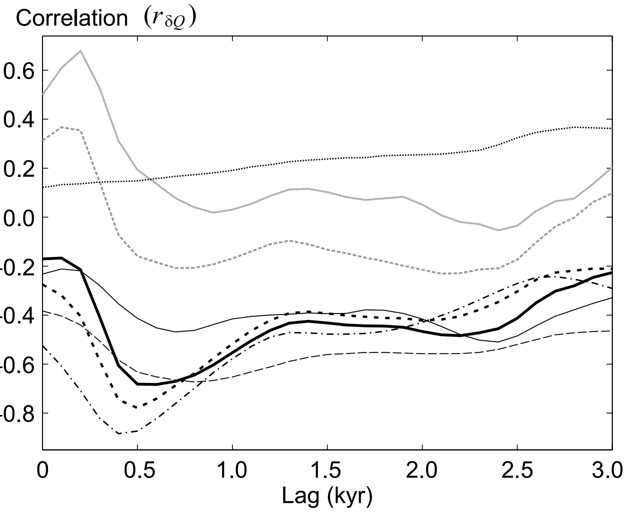

Figure 5. Lagged linear correlation coefficient between the climate forcing time series (GISP2 $\delta^{18}O$) and iceberg flux (Q) from select Northern Hemisphere coastal zones for the time period 60–20 kyr B.P., calculated for 100-year lags from 0 to 3000 years. Plotted are (from top to bottom at 0 lag) Barents/Kara Seas (gray solid line); Svalbard (grey dashed line); north Greenland (black dotted line); all circum-Atlantic sources (thick black line); Hudson Strait (thin black line); the North Pacific (thick dashed line); Labrador (long dashed line); and Scandinavia (dash-dotted line).

Greenland and little of this variability attributable to climate fluctuations.

3.2. Sensitivity of Results to the Climate Forcing

[28] We conducted additional experiments with only 50% of the D-O isotopic shift ascribed to temperature fluctuations. This has an interesting effect on the overall ice sheet evolution and a complex impact on modeled iceberg fluxes. Figure 6a presents the muted temperature variability in this experiment, as represented by the average air temperature over the North American and Eurasian ice sheets. Both interstadial and stadial periods are less extreme in this scenario (thick line in Figure 6a), inducing a markedly different ice sheet evolution. Because ice sheet mass balance is extremely sensitive to warm temperatures, the weaker interstadial events in the muted D-O scenario allow ice sheets in North America and Eurasia to grow to a greater LGM extent than in the reference model; warm periods are less intense and are unable to thwart the advance of ice.

[29] This also leads to subdued millennial-scale ice margin fluctuations (Figure 6b) and increased total iceberg efflux to the oceans during the glacial cycle (Table 3). Because the ice sheets have greater volume and are less prone to retreat, they spend more time advanced onto the continental shelf. Total iceberg fluxes increase by approximately 50% in most coastal zones. Midlatitude regions behave like the polar coastal zones of the reference model, with diminished climate sensitivity. Cold periods still lead to ice sheet advance and increased iceberg flux to the North Atlantic, with an overall circum-Atlantic response time of 600 years, as seen in the reference model (Table 3 and Figure 7). However, the response to cold periods is weakened to the degree that the brief flushing events during interstadial events become equally significant for the total circum-Atlantic iceberg flux. Overall, the millennial variability of iceberg fluxes is greatly diminished and the climatic control of iceberg flux is weaker.

[30] Because the phasing of iceberg fluxes from both North America and Eurasia under muted D-O cycles differs from that of the reference model, the qualitative results of these simulations need to be considered carefully. Millennial-scale IRD fluxes can still be anticipated with muted climatic variability. However, the stadial pulses of IRD that we predict with weaker D-O cycles would be set against a more steady background of IRD, which would make them less distinct in the sediment record.

4. Discussion

[31] The advance of ice during the cold phase of D-O cycles creates a succession of millennial-scale iceberg discharge cycles, with maximum iceberg flux to the North Atlantic predicted approximately 600 years into each stadial event. This echoes the millennial-scale IRD deposits seen in the North Atlantic [e.g., *Bond et al.*, 1993; *Grousset et al.*, 1993], the Nordic Seas [*Dowdeswell et al.*, 1999], and the Irminger Basin [*Elliot et al.*, 2001; *van Kreveld et al.*, 2000], which appear to correspond to the cold phase of D-O cycles [*Elliot et al.*, 1998, 2001; *Andrews and Barber*, 2002].

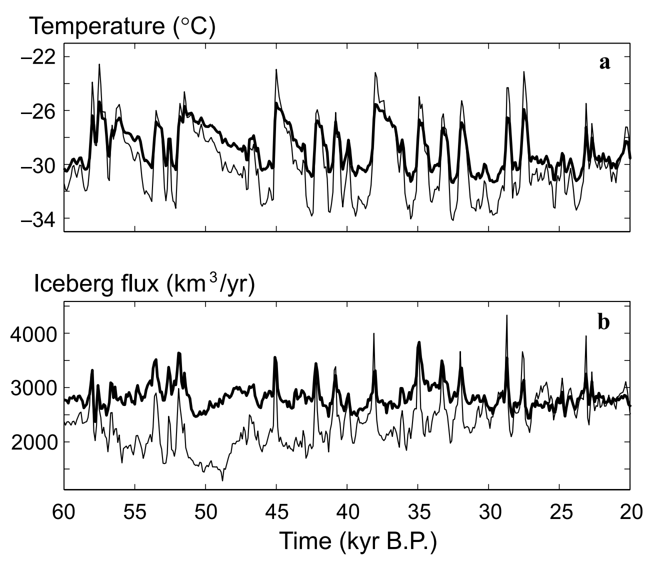

Figure 6. Sensitivity tests with muted Dansgaard-Oeschger (D-O) climate forcing: results for the period 60–20 kyr B.P. Thick lines indicate the muted D-O simulations, and thin lines indicate the reference model of Figure 2. (a) Average air temperature over the North American and Eurasia ice sheets (°C). (b) Iceberg flux to the North Atlantic, circum-Atlantic sources (km^3/yr).

Table 3. Iceberg Statistics as in Table 2 but With Muted Dansgaard-Oeschger Cycles

Coastal Zone	Total Iceberg Flux, 10^6 km^3	Normalized Flux, 10^3 km^2	$r_{\delta Q}$, 120 kyr	$r_{\delta Q}$ ($\tau = 0$), 60–20 kyr B.P.	$r_{\delta Q}$ (maximum), 60–20 kyr B.P.	Lag, year
North Pacific	94.3	35.4	−0.79	−0.52	−0.91	400
Canadian Arctic	29.3	9.1	−0.54	0.26	0.29	200
Baffin Bay	21.8	8.9	−0.62	0.20	0.21	100
Hudson Strait	25.6	76.9	−0.53	0.26	0.35	200
Labrador	23.7	26.6	−0.73	−0.27	−0.65	900
Southeast Laurentide	28.5	21.4	−0.49	0.17	0.39	2000
North Greenland	12.6	4.2	0.57	0.12	0.38	2200
South Greenland	15.8	6.3	−0.23	−0.11	0.26	2300
Iceland	2.6	1.9	−0.55	−0.25	−0.41	300
Great Britain	0.5	0.4	−0.12	0.14	0.14	0
Scandinavia	101.0	60.7	−0.72	−0.06	−0.59	500
Svalbard	29.2	21.9	−0.51	0.35	0.39	100
Barents/Kara Seas	8.6	4.1	0.29	0.33	0.52	200
Laptev/Siberian Seas	1.6	0.5	−0.11	−0.01	−0.30	800
Full North Atlantic	268.1	14.1	−0.65	0.26	−0.26	600

[32] This behavior is consistently predicted in our ice sheet simulations and is largely dominated by advance-retreat sequences on the marine margin of the Scandinavian Ice Sheet. Similar behavior is seen in most midlatitude coastal zones, with timescales of ice sheet response varying in each region as a function of the glaciological and climatic setting. Model results are not sensitive to the calving parameterization that we adopt; millennial-scale variability in iceberg fluxes is governed more by whether the ice sheet margin is advanced onto the continental shelf. On the timescales that we are analyzing, this is determined by the total flux of ice across the grounding line, which is dictated by ice marginal mass balance and the dynamical advance of ice in each region. Uncertainties in the calving parameterization are secondary to those associated with the overall climate forcing.

[33] Model resolution is inadequate to veraciously capture coastal fjord regions that channeled much of the coastal ice advance during stadial periods. Ice flux in the model is still concentrated in major outlet valleys (e.g., Hudson Strait, Cumberland Sound, Scoresby Sund), and for the reasons described above (overall ice marginal mass balance controls on ice advance), we are confident in the overall ice fluxes that are predicted from each coastal region. However, the model will predict a more spatially diffuse coastal flux than would be expected in Nature, and high-resolution modeling is needed to allow a comparison of modeled IRD with nearshore paleoceanographic records. Errors associated with poor resolution of outlet fjords will make our simulations conservative, as fjord environments increase iceberg delivery to the oceans and are also climatically sensitive [e.g., *Andrews et al.*, 1996, 1997; *Luckman and Murray*, 2005]. Indeed, we appear to underestimate the sensitivity of ice margins in southeast Greenland in our simulations, relative to paleoceanographic observations of millennial-scale IRD emanating from east Greenland [*van Kreveld et al.*, 2000]. This undersensitivity in the model reinforces our assertion that the millennial-scale iceberg variability that we predict is conservative.

[34] In the paleoceanographic record, millennial IRD layers in the East Greenland, Irminger and Nordic Seas are distinct from Heinrich layers and they dominate the IRD record in the these regions, with little or no input from the Laurentide Ice Sheet [*Elliot et al.*, 1998, 2001; *Dowdeswell et al.*, 1999]. In contrast, sediments from Heinrich events are dominant in the Labrador Sea [*Andrews and Tedesco*, 1992; *Andrews and Barber*, 2002] and the IRD belt [*Ruddiman*, 1977] of the North Atlantic [*Bond et al.*, 1992; *Grousset et al.*, 1993]. *Elliot et al.* [2001] demonstrate that periods of increased IRD delivery to the Nordic Seas

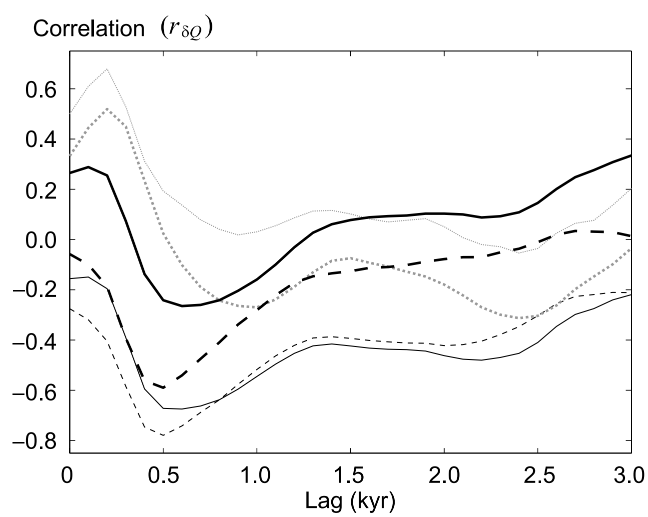

Figure 7. Lagged iceberg response for the period 60–20 kyr B.P. under muted D-O climate forcing. Thick lines indicate the muted D-O simulations, and thin lines indicate the reference model with full D-O forcing (compare Figure 5). Plotted are (from top to bottom at 0 lag) Barents/Kara Seas, full D-O forcing (thin grey dotted line); Barents/Kara Seas, muted D-O forcing (thick grey dotted line); all circum-Atlantic sources, muted D-O forcing (thick solid line); Scandinavia, muted D-O forcing (thick dashed line); all circum-Atlantic sources, full D-O forcing (thin solid line); and Scandinavia, full D-O forcing (thin dashed line).

are consistent with increased iceberg flux and not simply enhanced preservation of icebergs, although both effects may play a role.

[35] Our results resolve an outstanding issue regarding ice sheet behavior during the last glacial period. It is clear that the millennial IRD deposits originated nearly simultaneously from numerous circum-Atlantic sources, including ice sheets in eastern Greenland, Iceland, Scandinavia, Svalbard, and the Barents Sea. This has been interpreted as a climatically orchestrated instability in the circum-Atlantic ice sheets [*Bond et al.*, 1993], but this interpretation is difficult to reconcile with glaciological understanding of ice sheet surges or dynamical instabilities [*Clarke et al.*, 1999; *Dowdeswell et al.*, 1999; *Alley et al.*, 1999]. Surges are not subject to climatic triggers and would not occur simultaneously from different ice sheets or different sectors of an ice sheet. A synchronized climate-driven advance of the marine margins of the various ice sheets is more plausible to account for the millennial-scale IRD deposits [*Alley et al.*, 1999].

[36] The relative timing of IRD delivery from different ice sheets can be ascertained [*Bond and Lotti*, 1995; *Grousset et al.*, 2001; *Elliot et al.*, 2001], but absolute dating at submillennial timescales is difficult so the precise phasing with D-O cycles in the Greenland ice cores is unclear [*Andrews and Barber*, 2002]. On centennial timescales, the response of ice sheet margins to D-O climate forcing differs in each coastal region, so systematic depositional sequences can be expected. Near-coastal sites should witness an increase in locally derived IRD within 100 years of climate warming or cooling in most regions. For instance, Iceland responds quickly to cold phases and Icelandic IRD would appear first at sites proximal to Iceland. Further from local influences in the Nordic Seas and eastern North Atlantic, IRD may be dominated by sources from coastal Norway and the Barents Sea, based on the rapid response times and more dynamic ice sheets in these regions. Our simulations suggest that Norwegian-derived IRD would be expected to arrive first under a cooling, while Barents-derived IRD may peak following a warming event. An oceanographic model with iceberg trajectory and melt modeling is needed to simulate the detailed depositional sequence that one would expect in the open ocean or at a particular marine core site. On multicentury to millennial timescales, D-O driven icebergs from different circum-Atlantic sources would appear simultaneous.

[37] We argue that Heinrich events and D-O-driven icebergs reflect different glaciological processes. However, circum-Atlantic-derived IRD coincides with Heinrich (northeastern North American) sediments in the North Atlantic [e.g., *Bond and Lotti*, 1995; *Grousset et al.*, 2001]. We believe that the widespread cooling leading up to Heinrich events induced a broad mass balance driven advance of marine-based ice, similar to all other D-O cold phases. The climatic impact of Heinrich events may also have influenced the downstream ice sheets. The freshwater flux and North Atlantic cooling associated with the Hudson Strait icebergs induced a southward displacement of the polar front [*Vidal et al.*, 1997], which would have promoted preservation and transport of European-derived IRD to the midlatitude IRD belt.

[38] Cool mixed layer temperatures at these times would also have increased IRD delivery by sea ice transport. The Holocene record indicates that sea ice can play a significant role in IRD transport [*Bond et al.*, 2001], and that IRD fluctuations can occur even in the absence of significant iceberg fluxes. The results of *Bond et al.* [2001] probably reflect sea ice expansion and enhanced preservation of both sea ice and Greenlandic icebergs during cool periods of the Holocene. During glacial periods, and particularly during stadial events, expanded sea ice and enhanced preservation would add to the accentuated IRD transport caused by the high efflux of icebergs.

5. Conclusions About Ice Sheet Stability

[39] We argue for a distinction between IRD derived from ice sheet instabilities (Heinrich events) and that derived from large-scale climate (i.e., mass balance) fluctuations. Figures 2–4 should be interpreted as the ambient climate-driven flux of icebergs to the northern oceans. Our simulations indicate that this millennial-scale variability in iceberg fluxes is governed primarily by whether the ice sheet margin is advanced onto the continental shelf. This in turn is controlled by ice sheet history and, in the presence of mature ice sheets, by century- to millennial-scale climatic fluctuations.

[40] Ice sheets advance during cold periods, with peak iceberg fluxes predicted within 500 years of the cooling. Different coastal regions have different sensitivities to millennial climate variability, with relatively warm, wet climates (e.g., Scandinavia, western North America) exhibiting the highest millennial variability in iceberg flux and the most rapid response to D-O cycles.

[41] These results are independent of the iceberg calving parameterization that we adopt in our simulations; ice sheet flux across the grounding line is the first-order control on iceberg flux. This in turn is governed by ice dynamics and by the extent of ablation on the ice sheet margins. When it is warm enough that ablation drives a retreat of the ice sheet margin, iceberg fluxes decline. When ice dynamics and/or cooler climates permit ice advance onto the continental shelf, iceberg fluxes increase. In addition to this dominant mode of D-O driven iceberg variability, secondary peaks in iceberg flux occur as a result of “flushing” or collapse of marine-based ice sheets in the Barents Sea. These are rapid events, precipitated by millennial warming.

[42] Heinrich events will superimpose on these climate-driven ice fluxes as brief, extreme episodes that result from dynamical ice sheet destabilization. This difference between Heinrich events and D-O cycles has been broadly misunderstood in the paleoclimate community. The processes at play in triggering ice sheet dynamical instability in Hudson Strait remain open to debate. Heinrich events do not occur in our simulations; they do not arise spontaneously in the ice sheet model. This is a well-known shortcoming of current glaciological models. Thermally regulated surge cycles can be simulated [*MacAyeal*, 1993; *Marshall and Clarke*, 1997; *Calov et al.*, 2002] and are expected to occur

in ice sheets, but the numerical representation of ice streams in continental-scale ice sheet models is still under development. The main limitation is that the subglacial mechanisms governing glacier and ice sheet surges (basal hydrology, basal sediment deformation) are not fully understood and are absent or overly simplified in current ice sheet models [*Marshall et al.*, 2000]. This prohibits a diagnostic prediction of when and where ice streams or surges will arise in ice sheets.

[43] Our interpretation implies that dynamical ice sheet instabilities do occur, but they are infrequent, high-impact events that originated primarily (if not exclusively) in northeastern North America. Millennial cycles in IRD concentration and the co-coordinated delivery of IRD from a variety of ice sheet sources are most easily interpreted as advance/retreat sequences from circum-Atlantic marine margins, driven by large-scale climate (i.e., mass balance) fluctuations. Enhanced iceberg preservation during the cold phase of D-O cycles may also contribute to the marine IRD concentrations. We conclude that the sediment record contains evidence of intermittent ice sheet collapse as well as more frequent, mass balance controlled IRD releases from the ice sheet margins. The IRD record should not be interpreted as a proxy for millennial-scale ice sheet instability. This reconciles a long-standing confusion between the reaction of ice sheets to climatic change and their active role in delivering enormous quantities of ice to the North Atlantic during Heinrich events.

[44] If our interpretation is correct, it implies that ice sheet dynamical collapse occurred during the glaciation, but it was not commonplace: Only 4–6 IRD events during the last 60 kyr can be convincingly argued to be a result of ice sheet surges.

[45] The sea level impact of these events is still a matter of debate. While the quantities of IRD testify to large fluxes of ice [e.g., *Dowdeswell et al.*, 1995; *Alley and MacAyeal*, 1994; *Hemming*, 2004], more work is needed to constrain the amount of ice truly involved in a Heinrich event. Dramatic sea level impacts [*Chappell*, 2002] are difficult to conjure during cold parts of the glacial period. The cold temperatures that prevailed at the time of Heinrich events would have suppressed significant surface melt from the ice sheets, so even 2 m of sea level rise over a timescale of centuries can only be explained by large-scale surging or ice streaming activity [e.g., *MacAyeal*, 1993]. Glaciologically realistic surge simulations argue for more moderate sea level impacts [*Marshall and Clarke*, 1997], but glaciological models of ice streaming and surging physics need further development.

[46] Even the more modest sea level scenarios would pose a large societal impact if a similar event were to occur in Antarctica or Greenland. Further study of the North Atlantic sediment record and advances in ice sheet modeling are needed to assess the innate stability of ice sheets. Our simulations offer a predictive model for the sequence of IRD deposition in D-O cycles that can be tested by high-resolution paleoceanographic data. Because of the large sensitivity of our simulations to the magnitude of D-O climate fluctuations, we also believe that the IRD record can offer insight into the true severity of the fluctuations recorded in Greenland, as well as their geographical extent.

[47] **Acknowledgments.** Many of the ideas presented in this contribution stemmed from a University of Washington graduate seminar on Heinrich events, kindly organized by J. Jarvis, S. Rupper, G. Roe, and E. Steig. We acknowledge the support of the Sciences and Engineering Research Canada (NSERC), the Canadian Institute of Advanced Research, and a Fulbright Scholarship awarded to M.K. for a 12-month visit to the University of Calgary. Sincere thanks to M. Elliot and S. Hemming, whose thorough reviews improved this contribution.

References

Alley, R. B., and D. R. MacAyeal (1994), Ice-rafted debris associated with binge/purge oscillations of the Laurentide Ice Sheet, *Paleoceanography*, *9*(4), 503–511.

Alley, R. B., P. U. Clark, L. D. Keigwin, and R. S. Webb (1999), Making sense of millennial-scale climate change, in *Mechanisms of Global Climate Change at Millennial Time Scales*, *Geophys. Monogr. Ser.*, vol. 112, edited by P. U. Clark, R. S. Webb, and L. D. Keigwin, pp. 385–394, AGU, Washington D. C.

Alley, R. B., S. Anandakrishnan, and P. Jung (2001), Stochastic resonance in the North Atlantic, *Paleoceanography*, *16*(2), 190–198.

Andrews, J. T., and D. C. Barber (2002), Dansgaard-Oeschger events: Is there a signal off the Hudson Strait ice stream?, *Quat. Sci. Rev.*, *21*, 443–454.

Andrews, J. T., and K. Tedesco (1992), Detrital carbonate-rich sediments, northwestern Labrador Sea: Implications for ice-sheet dynamics and iceberg rafting (Heinrich) events in the North Atlantic, *Geology*, *20*, 1087–1090.

Andrews, J. T., H. Erlenkeuser, K. Tedesco, A. E. Aksu, and A. J. T. Jull (1994), Late Quaternary (stage 2 and 3) meltwater and Heinrich events, northwest Labrador Sea, *Quat. Res.*, *41*, 26–34.

Andrews, J. T., A. E. Jennings, T. Cooper, K. M. Williams, and J. Mienert (1996), Late Quaternary sedimentation along a fjord to shelf (trough) transect, East Greenland (c.68°N), in *Late Quaternary Paleoceanography of the North Atlantic Margins*, edited by J. T. Andrews et al., *Geol. Soc. Spec. Publ. London*, *111*, 153–166.

Andrews, J. T., L. M. Smith, R. Preston, T. Cooper, and A. E. Jennings (1997), Holocene patterns of ice-rafted detritus (IRD) in cores from the East Greenland shelf, *J. Quat. Sci.*, *12*, 1–13.

Björnsson, H., F. Pálsson, O. Sigurdsson, and G. E. Flowers (2003), Surges of glaciers in Iceland, *Ann. Glaciol.*, *36*, 82–90.

Bond, G., and R. Lotti (1995), Iceberg discharges into the North Atlantic on millennial time scales during the last glaciation, *Science*, *267*, 1005–1010.

Bond, G. C., et al. (1992), Evidence of massive discharges of icebergs into the North Atlantic Ocean during the last glacial period, *Nature*, *360*, 245–249.

Bond, G., W. S. Broecker, S. Johnsen, J. McManus, L. Labeyrie, J. Jouzel, and G. Bonani (1993), Correlations between climate records from North Atlantic sediments and Greenland ice, *Nature*, *365*, 143–147.

Bond, G., et al. (2001), Persistent solar influence on North Atlantic climate during the Holocene, *Science*, *294*, 2130–2136.

Broecker, W. S. (1994), Massive iceberg discharges as triggers for global climate change, *Nature*, *372*, 421–424.

Broecker, W. S., and S. Hemming (2001), Paleoclimate-climate swings come into focus, *Science*, *294*, 2308–2309.

Calov, R., A. Ganopolski, V. Petoukhov, and M. Claussen (2002), Large-scale instabilities of the Laurentide ice sheet simulated in a fully coupled climate-system model, *Geophys. Res. Lett.*, *29*(24), 2216, doi:10.1029/2002GL016078.

Chappell, J. (2002), Sea-level changes forced ice breakouts in the Last Glacial cycle: New results from coral terraces, *Quat. Sci. Rev.*, *21*, 1229–1240.

Church, J. A., and J. M. Gregory (2001), Changes in sea level, in *Climate Change 2001: The Scientific Basis*, edited by J. T. Houghton et al., pp. 639–693, Cambridge Univ. Press, New York.

Clark, P. U., N. G. Pisias, T. F. Stocker, and A. J. Weaver (2002), The role of thermohaline circulation in abrupt climate change, *Nature*, *415*, 863–869.

Clarke, G. K. C. (1987), Fast glacier flow: Ice streams, surging, and tidewater glaciers, *J. Geophys. Res.*, *92*, 8835–8841.

Clarke, G. K. C., S. J. Marshall, C. Hillaire-Marcel, G. Bilodeau, and C. Veiga-Pires (1999), A glaciological perspective on Heinrich events, in *Mechanisms of Global Climate Change at Millennial Time Scales*, *Geophys. Monogr. Ser.*, vol. 112, edited by P. U. Clark, R. S. Webb, and L. D. Keigwin, pp. 243–262, AGU, Washington, D. C.

Cortijo, E., L. Labeyrie, L. Vidal, M. Vautravers, M. Chapman, J.-C. Duplessy, M. Elliot, M. Arnold, J.-L. Turon, and G. Auffret (1997), Changes in sea surface hydrology associated with Heinrich event 4 in the North Atlantic Ocean between 40° and 60°N, *Earth Planet. Sci. Lett.*, *146*, 29–45.

Dansgaard, W., et al. (1993), Evidence for general instability of past climate from a 250-kyr ice core record, *Nature*, *364*, 218–220.

Denton, G. H., R. B. Alley, G. C. Comer, and W. S. Broecker (2005), The role of seasonality in abrupt climate change, *Quat. Sci. Rev.*, *24*, 1159–1182.

Dokken, T. M., and E. Jansen (1999), Rapid changes in the mechanism of ocean convection during the last glacial period, *Nature*, *401*, 458–461.

Dowdeswell, J. A., M. A. Maslin, J. T. Andrews, and I. N. McCave (1995), Iceberg production, debris rafting, and the extent and thickness of Heinrich layers (H-1, H-2) in North Atlantic sediments, *Geology*, *23*, 301–304.

Dowdeswell, J. A., A. Elverøi, J. T. Andrews, and D. Hebbeln (1999), Asynchronous deposition of ice-rafted layers in the Nordic Seas and North Atlantic Ocean, *Nature*, *400*, 348–351.

Elliot, M., L. Labeyrie, G. Bond, E. Cortijo, J.-L. Turon, N. Tisnerat, and J.-C. Duplessy (1998), Millennial-scale iceberg discharges in the Irminger Basin during the last glacial period: Relationship with the Heinrich events and environmental settings, *Paleoceanography*, *13*(5), 433–446.

Elliot, M., L. Labeyrie, T. Dokken, and S. Manthé (2001), Coherent patterns of ice-rafted debris deposits in the Nordic regions during the last glacial (10–60 ka), *Earth Planet. Sci. Lett.*, *194*, 151–163.

Elliot, M., L. Labeyrie, and J. C. Duplessy (2002), Changes in North Atlantic deep-water formation associated with the Dansgaard-Oeschger temperature oscillations (10–60 ka), *Quat. Sci. Rev.*, *21*, 1153–1165.

Farmer, G. L., D. C. Barber, and J. T. Andrews (2003), Provenance of late Quaternary ice proximal sediments in the North Atlantic: Nd, Sr and Pb isotopic evidence, *Earth Planet. Sci. Lett.*, *209*, 227–243.

Francois, R., and M. Bacon (1994), Heinrich events in the North Atlantic: Radiochemical evidence, *Deep Sea Res., Part I*, *41*(2), 315–334.

Gregory, J. M., and J. Oerlemans (1997), Simulated future sea-level rise due to glacier melt based on regionally and seasonally resolved temperature changes, *Nature*, *391*, 474–476.

Grootes, P. M., M. Stuiver, J. W. C. White, S. J. Johnsen, and J. Jouzel (1993), Comparison of oxygen isotope records from GISP2 and GRIP Greenland ice cores, *Nature*, *366*, 552–554.

Grousset, F. E., L. Labeyrie, J. A. Sinko, M. Cremer, G. Bond, J. Duprat, E. Cortijo, and S. Huon (1993), Patterns of ice-rafted detritus in the glacial North Atlantic (40–55°N), *Paleoceanography*, *8*(2), 175–192.

Grousset, F. E., E. Cortijo, S. Huon, L. Hervé, T. Richter, D. Burdloff, J. Duprat, and O. Weber (2001), Zooming in on Heinrich layers, *Paleoceanography*, *16*(3), 240–259.

Gwiazda, R. H., S. R. Hemming, and W. S. Broecker (1996a), Tracking the sources of icebergs with lead isotopes: The provenance of ocean-rafted debris in Heinrich Layer 2, *Paleoceanography*, *11*, 77–93.

Gwiazda, R. H., S. R. Hemming, and W. S. Broecker (1996b), Provenance of icebergs during Heinrich event 3 and the contrast to their sources during other Heinrich episodes, *Paleoceanography*, *11*(4), 371–378.

Heinrich, H. (1988), Origin and consequences of cyclic ice rafting in the northeast Atlantic Ocean during the past 130,000 years, *Quat. Res.*, *29*, 142–152.

Hemming, S. (2004), Heinrich events: Massive late Pleistocene detritus layers of the North Atlantic and their global climate imprint, *Rev. Geophys.*, *42*, RG1005, doi:10.1029/2003RG000128.

Hemming, S. R., W. S. Broecker, W. D. Sharp, G. C. Bond, R. H. Gwiazda, J. F. McManus, M. Klas, and I. Hajdas (1998), Provenance of Heinrich layers in core V28–82, northeastern Atlantic: ^{40}Ar-^{39}Ar ages of ice-rafted hornblende, Pb isotopes in feldspar grains, and Nd-Sr-Pb isotopes in the fine sediment fraction, *Earth Planet. Sci. Lett.*, *164*, 317–333.

Hemming, S. R., C. M. Hall, P. E. Biscaye, S. M. Higgins, G. C. Bond, J. F. McManus, D. C. Barber, J. T. Andrews, and W. S. Broecker (2002), ^{40}Ar/^{39}Ar ages and ^{40}Ar* concentrations of fine-grained sediment fractions from North Atlantic Heinrich layers, *Chem. Geol.*, *182*, 583–603.

Hillaire-Marcel, C., A. de Vernal, G. Bilodeau, and G. Wu (1994), Isotope stratigraphy, sedimentation rates, deep circulation, and carbonate events in the Labrador Sea during the last ~200 kyr, *Can. J. Earth Sci.*, *31*, 68–89.

Huybrechts, P., and J. de Wolde (1999), The dynamic response of the Antarctic and Greenland ice sheets to multiple-century climatic warming, *J. Clim.*, *12*, 2169–2188.

Johnsen, S. J., et al. (1992), Irregular glacial interstadials recorded in a new Greenland ice core, *Nature*, *359*, 311–312.

Keigwin, L. D., G. A. Jones, S. J. Lehman, and E. A. Boyle (1991), Deglacial meltwater discharge, North Atlantic deep circulation and abrupt climate change, *J. Geophys. Res.*, *96*, 16,811–16,826.

Li, C., D. S. Battisti, D. P. Schrag, and E. Tziperman (2005), Abrupt climate shifts in Greenland due to displacements of the sea ice edge, *Geophys. Res. Lett.*, *32*, L19702, doi:10.1029/2005GL023492.

Lowell, T. V., C. J. Heusser, C. Schluchter, D. R. Marchant, and G. H. Denton (1995), Interhemispheric correlation of late Pleistocene glacial events, *Science*, *269*, 1541–1549.

Luckman, A., and T. Murray (2005), Seasonal variation in velocity before retreat of Jakobshavn Isbræ, Greenland, *Geophys. Res. Lett.*, *32*, L08501, doi:10.1029/2005GL022519.

MacAyeal, D. R. (1993), Binge/purge oscillations of the Laurentide ice sheet as a cause of the North Atlantic's Heinrich events, *Paleoceanography*, *8*(6), 775–784.

Marshall, S. J., and G. K. C. Clarke (1997), A continuum mixture model of ice stream thermomechanics in the Laurentide Ice Sheet, 2. Application to the Hudson Strait Ice Stream, *J. Geophys. Res.*, *102*, 20,615–20,638.

Marshall, S. J., and K. M. Cuffey (2000), Peregrinations of the Greenland Ice Sheet divide through the last glacial cycle and implications for disturbance of central Greenland ice cores, *Earth Planet. Sci. Lett.*, *179*, 73–90.

Marshall, S. J., L. Tarasov, G. K. C. Clarke, and W. R. Peltier (2000), Glaciological reconstruction of the Laurentide Ice Sheet: Physical processes and modelling challenges, *Can. J. Earth Sci.*, *37*, 769–793.

Marshall, S. J., T. S. James, and G. K. C. Clarke (2002), North American Ice Sheet reconstructions at the Last Glacial Maximum, *Quat. Sci. Rev.*, *21*, 175–192.

McCabe, A. M., and P. U. Clark (1998), Ice sheet variability around the North Atlantic Ocean during the last deglaciation, *Nature*, *392*, 373–377.

McManus, J. F., R. F. Anderson, W. S. Broecker, M. Q. Fleisher, and S. M. Higgins (1998), Radiometrically determined sedimentary fluxes in the sub-polar North Atlantic during the last 140,000 years, *Earth Planet. Sci. Lett.*, *155*, 29–43.

McManus, J. F., R. Francois, J.-M. Gherardi, L. D. Keigwin, and S. Brown-Leger (2004), Collapse and rapid resumption of the Atlantic meridional circulation linked to deglacial climate changes, *Nature*, *428*, 834–837.

Ohmura, A., M. Wild, and L. Bengtsson (1996), A possible change in mass balance of Greenland and Antarctic ice sheets in the coming century, *J. Clim.*, *9*, 2124–2135.

Parizek, B. R., and R. B. Alley (2004), Implications of increased Greenland surface melt under global-warming scenarios: Ice-sheet simulations, *Quat. Sci. Rev.*, *23*, 1013–1027.

Porter, S. C., and Z. S. An (1995), Correlation between climate events in the North Atlantic and China during the last glaciation, *Nature*, *375*, 305–308.

Rahmstorf, S. (2002), Ocean circulation and climate during the past 120,000 years, *Nature*, *419*, 207–214.

Rignot, E., G. Casassa, P. Gogineni, W. Krabill, A. Rivera, and R. Thomas (2004), Accelerated ice discharge from the Antarctic Peninsula following the collapse of Larsen B ice shelf, *Geophys. Res. Lett.*, *31*, L18401, doi:10.1029/2004GL020697.

Roche, D., D. Paillard, and E. Cortijo (2004), Constraints on the duration and freshwater release of Heinrich event 4 through isotope modelling, *Nature*, *432*, 379–382.

Rohling, E., R. Marsh, N. C. Wells, M. Siddall, and N. R. Edwards (2004), Similar meltwater contributions to glacial sea level changes from Antarctica and northern ice sheets, *Nature*, *430*, 1016–1021.

Ruddiman, W. (1977), Late Quaternary deposition of ice-rafted sand in the subpolar North Atlantic (lat 40 to 65 N), *Geol. Soc. Am. Bull.*, *88*, 1813–1827.

Scambos, T. A., C. L. Hulbe, M. A. Fahnestock, and J. Bohlander (2000), The link between climate warming and ice shelf breakups in the Antarctic Peninsula, *J. Glaciol.*, *46*(154), 516–530.

Severinghaus, J., and E. Brook (1999), Abrupt climate change at the end of the last glacial period inferred from trapped air in polar ice, *Science*, *286*, 930–934.

Siddall, M., E. J. Rohling, A. Almogi-Labin, C. Hemleben, S. Meischner, I. Schmelzer, and D. A. Smeed (2003), Sea-level fluctuations during the last glacial cycle, *Nature*, *423*, 853–858.

Snoeckx, H., F. E. Grousset, M. Revel, and A. Boelaert (1999), European contribution of ice-

rafted sand to Heinrich layers H3 and H4, *Mar. Geol.*, *158*, 197–208.
Stoner, J. S., J. E. T. Channell, and C. Hillaire-Marcel (1998), A 200 ka geomagnetic chronostratigraphy for the Labrador Sea: Indirect correlation of the sediment record to SPECMAP, *Earth Planet Sci. Lett.*, *159*, 165–181.
Thompson, J., N. C. Higgs, and T. Clayton (1995), A geochemical criterion for the recognition of Heinrich events and estimation of their depositional fluxes by the $^{230}Th_{excess}$ profiling method, *Earth Planet. Sci. Lett.*, *135*, 41–56.
van Kreveld, S., M. Sarnthein, H. Erlenkeuser, P. Grootes, S. Jung, M. J. Nadeau, U. Pflaumann, and A. Voelker (2000), Potential links between surging ice sheets, circulation changes, and the Dansgaard-Oeschger cycles in the Irminger Sea, 60–18 kyr, *Paleoceanography*, *15*(4), 425–442.
Vaughan, D. G., and C. S. M. Doake (1996), Recent atmospheric warming and retreat of ice shelves on the Antarctic Peninsula, *Nature*, *379*, 328–331.
Veiga-Pires, C. C., and C. Hillaire-Marcel (1999), U and Th isotope constraints on the duration of Heinrich events H0–H4 in the southeastern Labrador Sea, *Paleoceanography*, *14*(2), 187–199.
Vettoretti, G., W. R. Peltier, and N. A. McFarlane (2000), Global water balance and atmospheric water vapour transport at Last Glacial Maximum: Climate simulations with the CCCma atmospheric general circulation model, *Can. J. Earth Sci.*, *37*, 695–723.
Vidal, L., et al. (1997), Evidence for changes in the North Atlantic Deep Water linked to meltwater surges during the Heinrich events, *Earth Planet. Sci. Lett.*, *146*, 13–27.
Voelker, A. H. L. (2002), Global distribution of centennial-scale records for marine isotope stage (MIS) 3: A database, *Quat. Sci. Rev.*, *21*, 1185–1212.
Zahn, R., J. Schönfeld, H. R. Kudrass, M. H. Park, H. Erlenkeuser, and P. Grootes (1997), Thermohaline instability in the north Atlantic during meltwater events: Stable isotope and ice-rafted detritus records from core SO75–26KL, Portuguese margin, *Paleoceanography*, *12*(5), 696–710.
Zwally, J. H., W. Abdalati, T. Herring, K. Larson, J. Saba, and K. Steffen (2004), Surface melt-induced acceleration of Greenland Ice Sheet flow, *Science*, *297*, 218–222.

M. R. Koutnik, Department of Earth and Space Sciences, University of Washington, Box 351310, Seattle, WA 98195, USA. (mkoutnik@u.washington.edu)
S. J. Marshall, Department of Geography, University of Calgary, 2500 University Drive NW, Calgary, Alberta, Canada T2N 1N4. (shawn.marshall@ucalgary.ca)